International Journal of Biomedicine 12(4) (2022) 493-505
http://dx.doi.org/10.21103/Article12(4)_RA1

REVIEW ARTICLE

INTERNATIONAL JOURNAL OF BIOMEDICINE

Leading–Edge Portable Biosensors and Biomarkers Development for Raman Biospectroscopy and Imaging in Cancer Diagnosis

Alireza Heidari[1,2,3,4*], Zahra Torfeh[5], Sophia Iorgulescu[1,2,3], Olivia Robinson[1,2,3], Lin Hu[1,2,3], Charlotte Vauclin[1,2,3], Ntalie Schiltz[1,2,3], Scarlett Sondermann[1,2,3], Lucy MacLennan[1,2,3], Julia Smith[1,2,3], Lydia Williamson[1,2,3]

[1]*Faculty of Chemistry, California South University, Irvine, CA, USA*
[2]*BioSpectroscopy Core Research Laboratory (BCRL), California South University, Irvine, CA, USA*
[3]*Cancer Research Institute (CRI), California South University, Irvine, CA, USA*
[4]*American International Standards Institute (AISI), Irvine, CA, USA*
[5]*An Independent Volunteer and Unaffiliated Researcher*

Graphical Abstract

Raman spectroscopy is an important method for identifying molecules, which is widely used in determining the chemical and structural characteristics of various substances. Many materials have a special Raman spectrum, so that this phenomenon has turned the Raman device into an efficient tool for studying the structural and chemical properties of molecules. Since it is possible to obtain detailed information about the chemical and structural characteristics of biological compounds from Raman spectroscopy, the use of this method is rapidly expanding in the field of life sciences, especially in biological and medical studies. There is no need for special, time–consuming and expensive preparations in the study of materials with the help of a Raman device. In the protein Raman spectrum, distinct bands arise from the vibrational states of the peptide backbone and amino acid side chains. Therefore, based on the position and intensity of the protein's Raman spectrum, it is possible to obtain valuable information about its second, third, and fourth structures. Also, the Raman spectrum of the protein contains information about the orientation and surrounding environment of the amino acid side chains. The correct formation of the disulfide bond in the protein structure can also be studied with the help of the Raman device. In general, the Raman spectrum of proteins contains multiple discrete bands that represent the vibrational states of the molecule and is used as a selective fingerprint to accurately determine the three–dimensional structure of proteins, intramolecular dynamics, and intermolecular interactions.

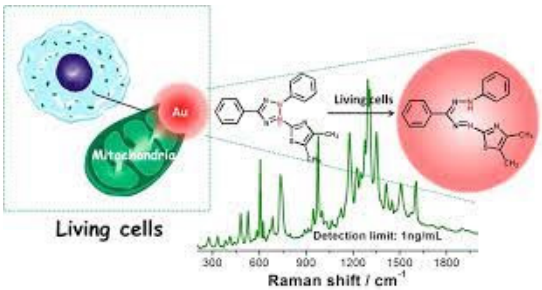

Schematic of leading–edge portable biosensors and biomarkers development for Raman biospectroscopy and imaging in cancer diagnosis.

Keywords: biosensors • biomarkers • Raman biospectroscopy • imaging • cancer • diagnosis

For citation: Heidari A, Torfeh Z, Iorgulescu S, Robinson O, Hu L, Vauclin C, Schiltz N, Sondermann S, MacLennan L, Smith J, Williamson L. Leading–Edge Portable Biosensors and Biomarkers Development for Raman Biospectroscopy and Imaging in Cancer Diagnosis. International Journal of Biomedicine. 2022;12(4):493-505. doi:10.21103/Article12(4)_RA1.

Introduction

The application of Raman spectroscopy is basically in the identification of molecules. Today, along with the many advances that have been made in the field of research equipment design, Raman spectroscopy has become more simple, accessible and affordable. Of course, despite the many advances made, the interpretation of Raman spectra is still a big challenge and requires special skills. Like all spectroscopic methods, the Raman spectrum contains information about the electromagnetic waves hitting the sample. After the electromagnetic beam hits the molecule, a part of it is scattered in all directions. Raman spectroscopy is used to observe vibrational, rotational, and other low-frequency states in a system. This type of spectroscopy typically provides a specific structural fingerprint that can be used to identify different molecules. In fact, this type of spectroscopy is based on inelastic scattering called Raman scattering (and the Raman light rays are usually laser light in the visible region, near infrared light or near ultraviolet light.[1–38]

The inelastic scattering of light upon impact with matter was not reported until 1928, while this important physical phenomenon was first predicted by Adolf Schmal in 1923. Also, Chandrasekhara Venkata Raman observed this effect for the first time after studying the passage of sunlight through organic solutions, and in 1930 he was honored to receive the Nobel Prize in Physics due to this important discovery and his other studies in this field. The development and evolution of this physical effect was carried out by George Pleczyk between 1930 and 1934. Also, in 1899, John William Reilly was able to justify the elastic scattering of light while proposing a new hypothesis. This light scattering theory was actually an answer to why the color of the sky is blue. At that time, light scattering studies were also seriously pursued in countries such as Russia, France, India, the United States of America, and Germany. In the early 20th century, people like Raman and Krishnan in India and Landsberg and Mandelstam in Russia were pioneers in this field of study. When investigating the change in the frequency of scattered light in different physical conditions, these people achieved results that they had not planned for in advance. Landsberg and Mandelstam also investigated the scattering of light in quartz and some other crystals to find the scattered rays that have undergone a frequency change compared to the incoming light. At the same time, Raman and Krishnan in India and far away from Russian scientists were studying the changes of light in the Compton effect. By publishing three articles in 1928, they recorded the change in the frequency of scattered light while encountering matter, even though the reports of Raman and Krishnan were only slightly earlier than the reports of Russian scientists. Nowadays, extensive studies are carried out on the scattering of light while interacting with matter, and the large volume of studies and the number of published scientific articles about this discovery show the special importance of this issue.[39–76]

Photons are often reflected, absorbed or scattered while hitting the molecule. In Raman spectroscopy, monochromatic light photons (light of a single wavelength) are scattered in different directions after hitting the sample. In fact, in Raman spectroscopy, photons scattered from the sample are important. Most of the photons that hit the molecule are scattered elastically. This type of scattering is called Rayleigh scattering, in which the photons scattered from the sample have the same energy or wavelength as the photons that hit the sample. In 1928, Indian physicist Chandra Sekhar Venkata Raman discovered the Raman phenomenon. In this phenomenon, the energy or wavelength of the beam scattered by the molecules is different from the wavelength of the primary beam that hits the sample. This type of scattering of light rays is called inelastic scattering. About one in ten million photons after hitting matter is scattered inelastically. Also, the amount of difference in energy or wavelength of inelastic scattered light depends on the molecular structure of the compound. In fact, Raman spectroscopy was formed based on the analysis of these differences and with the aim of determining the molecular structure of various compounds. The change in the wavelength or the initial radiation energy provides very important information about the molecular movements within the system. In Raman scattering, the photon collides with the material and after scattering its wavelength goes to the longitudinal direction. In these more or less displaced waves, the type of radiation scattering is dominated by the transmission to longer wavelengths, which is called Stokes Raman scattering. Also, the transition to lower wavelengths is called Raman anti–Stoke scattering. It has been reported that the intensity ratio of anti–Stoke to stoke scattering increases with increasing temperature. In fact, the incoming photon collides with the electron cloud of bonds of functional groups and excites the electrons to a virtual state. Then the electron returns from the virtual state to an excited vibrational or rotational state. This phenomenon causes the photon to lose some of its energy and is revealed in the form of Stokes Raman scattering. The lost energy is directly related to the chemical identity of the functional group, the molecular structure attached to it, the type of atoms in the molecule and its surrounding environment. Therefore, the Raman spectrum of each molecule is specific and can be used like a "fingerprint" to detect the chemical identity of molecular compounds in a liquid, on a surface, or in the air. [77–114]

Leading–Edge Portable Biosensors and Biomarkers Development

The degree of the Raman effect is directly related to the polarizability of the electrons of the molecule. The Raman effect is actually the interaction between the electron cloud of the sample and the external electric field of the incoming light rays. This mode creates the formation of which depends on the induced instantaneous dipole polarizability of the sample. Because the laser light does not excite the molecule, no actual transitions between energy levels occur in Raman studies. (with fluctuations, hence the Raman signal is obtained from the collision of the light beam (intermolecular photons (phonons) of the sample). Review and analysis of the information obtained in Raman spectroscopy to determine the structure, qualitative measurement, and in some cases, it takes a few molecules. Also, the study of the effect of many different physical parameters such as temperature, pressure and tension on interatomic and intermolecular oscillations. The Raman scattering spectrum and the infrared absorption spectrum of a molecule have many similarities with each other. In fact, it comes from the similarities

of these two methods. Also, despite the great similarity, these two methods are different from each other in the basic principles, so that they are usually used as complementary methods. In infrared absorption, the amount the energy absorbed from the incoming photon corresponds to the energy difference between the initial and final rotational–vibrational states, while in Raman scattering, the amount of energy of the incoming photon is not the same as the outgoing one (usually it is more or less). Also, the dependence of Raman on polarization the acceptability of its electric dipole–dipole species from infrared spectroscopy, which only observes dipole species. E is electric dependent (atomic polar tensor) differentiates. These differences indicate that transitions between rotational–vibrational states may not be active in infrared absorption, but can be studied using Raman spectroscopy. There is also the reverse of this phenomenon, so that infrared absorption spectroscopy is used in cases where Raman spectroscopy is not applicable for the study of molecules. Therefore, transitions that have a high intensity in the Raman spectrum often have weak infrared absorption and vice versa. In other words, a vibration is active in infrared spectroscopy, when a change in the momentary dipole of the molecule can be seen during its occurrence. Likewise, vibration is active in Raman spectroscopy, which changes the polarizability of the molecule as well. For example, molecules with identical nuclei, such as N2, H2, and O2 are active in the Raman study, but not active in infrared spectroscopy. In the CO2 molecule, the symmetric vibrational motion is active in Raman and not active in infrared. On the contrary, asymmetric vibrational motion is not active in Raman, but it is active in infrared. Some vibrations are also active in both infrared and Raman.

The main components of the Raman device, the system of each Raman device consists of four main parts, including the laser light source, the wavelength selector (sample illumination filter and light collecting lenses. After the light and the detector or spectrometer collide) the laser to the sample and Its scattering from its surface, the scattered light is collected by a lens and transmitted to the detector unit by a fiber. Wavelengths close to the laser wavelength (elastic or Rayleigh scattering) are absorbed by a special filter. Only the scattered rays that have changed in terms of energy or wavelength compared to the incoming light are allowed to pass and reach the detector.

The most common sources of laser generation in the Raman device are argon laser with wavelengths of 488 and 514.5 nm, krypton laser with wavelengths of 530, 568, and 647 nm, helium/neon laser with a wavelength of 632.8 nm, diode laser, with 785 and 830 nm wavelength and AG Y/d N laser with 1064 nm wavelength. The waves that change the frequency (wavelength) after hitting the sample while scattering are the Raman signals that are of special importance. The cross-section of Raman scattering is very small, and the most difficult step in this method is to separate the Rayleigh elastic beams from the frequency–shifted Raman beams known as inelastic beams. In the past, holographic gratings and multiple stages were used to obtain a high degree of Raman signal, which made the collection time relatively long. Today, notch filters or edge filters and spectrographs (or spectrometry on the axial transmitter), Zarni–Turner splitter for amplification, and detectors of the coupled device based on the Fourier transform of the Raman signal are used.

Results and Discussion

Raman, as mentioned earlier, Raman spectroscopy is widely used in various fields. In recent years, the use of Raman spectroscopy in medicine, pharmacy, food industry, defense science, and other industries has grown significantly. According to the global events of recent years, it is very important to establish methods for rapid detection of biological threats for the military and national security. In the meantime, Raman spectroscopy has received a lot of attention because it provides accurate and fast information about the molecular composition of biological materials in a non–destructive way. Currently, Raman spectroscopy is used to detect explosives, agents of chemical and bacterial warfare, and other dangerous chemical substances. With the help of this method, samples can be checked in a non–contact and non–destructive way inside transparent or semi-transparent packaging. Therefore, drugs and narcotics can be checked through the plastic bag containing them, and in this way, damage to criminal documents and evidence or their contamination can be avoided. It is also possible to equip a Raman spectroscopy probe with an optical fiber in order to measure nitrate, nitrite and hydroxide in tanks containing radioactive waste. These three chemicals are often used to display and control tank corrosion. In this way, there is no need to physically remove the sample from the tanks and the risks of transporting it to a fixed laboratory to check them. The accuracy of Raman detection depends on various factors, including the laser wavelength used and the type of material. The detection accuracy of these method variables usually ranges from a few parts per million to a few parts per billion. Raman's ability to display stress and other parameters, such as the surface temperature of the component, makes it an effective tool in the manufacture of semiconductor components. Also, the ability of this method to provide accurate images of cells allows comparison between healthy and diseased tissues, which is especially important in the study of cancerous tissues (Figures 1–5).

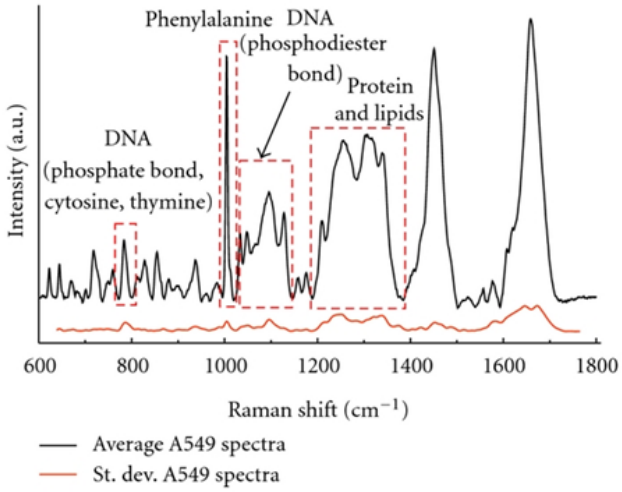

Fig. 1. *Raman spectroscopy investigation of DNA, protein and lipids in human cancer cells.*

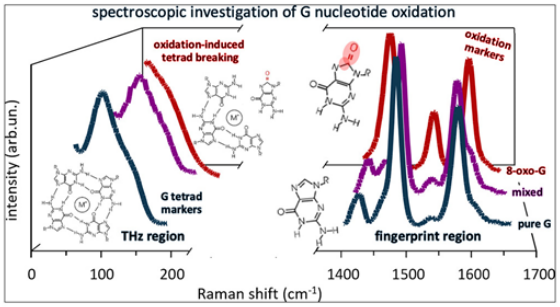

Fig. 2. Raman spectroscopy investigation of G nucleotide oxidation in human cancer cells.

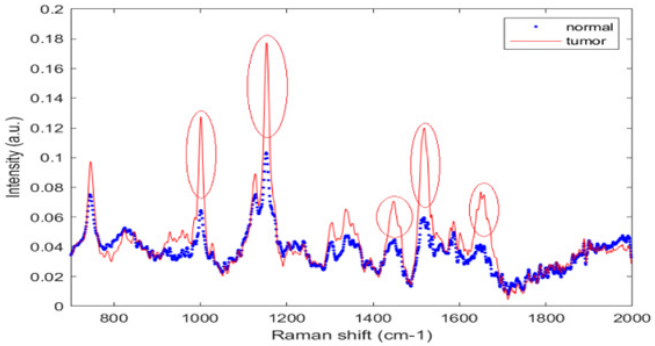

Fig. 3. Raman spectroscopy comparison between normal and cancer animal cells.

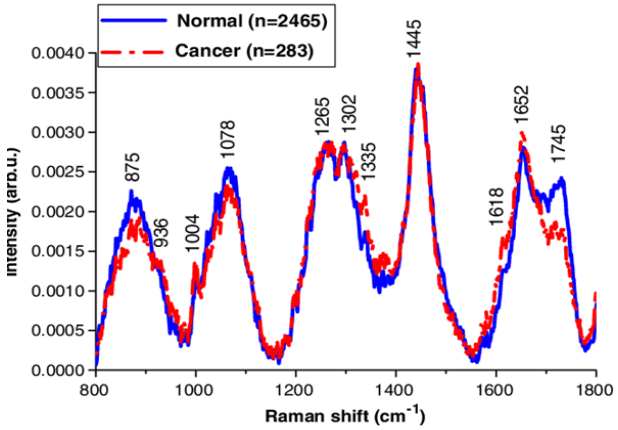

Fig. 4. Raman spectroscopy comparison between normal and cancer human cells.

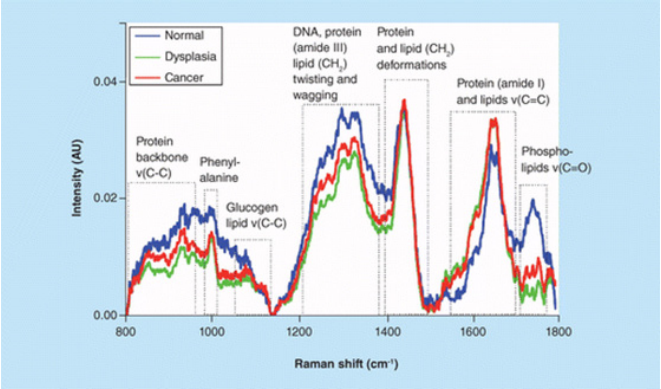

Fig. 5. Raman spectroscopy comparison among normal, dysplasia and cancer human cells.

What information can be obtained from examining the Raman scattering spectrum of materials? The vibrational frequencies of a link are very sensitive to the details and the structural features and local environment of the molecule, such as crystal phase symmetry, polymer morphology, and band position in the Raman spectrum representing the chemical species, crystal phase, or substance under study. The composition or compounds that make up the alloy, as well as the intensity of the Raman spectrum, indicates the concentration of the active group present in the composition or substance under investigation. Raman frequency shift indicates the type of functional group and temperature changes in the investigated substance. And finally, the width of the Raman spectrum indicates the presence of a disorder or structural disorder in the studied material.

Effect of solvent on the Raman spectrum of the protein. Protein in solution has a wider Raman spectrum than in powder form. The Raman spectrum of lysozyme protein in both powder and solution states. The type III amide bands of the protein in the solution state have a wider spectrum. The effect of chemical reactions on the folding and Raman spectrum of proteins in the presence of a concentration of different methanol amide bonds of type (I) alpha-synuclein protein have been modified and a detailed examination of this area after separating the sub–spectral surface, it is clear that the structure of alpha–synuclein protein under the influence of methanol gradually deviates from the normal state and in that second structures from alpha helix to structures called beta sheets and structures. The effect of reducing agents on the folding of proteins and its display in the Raman spectrum, after deconvolution of the protein Raman spectra, the amount of structural changes in the presence of reducing agents is determined. Physics such as reaction rate, free enthalpy and activation energy can be calculated from these data. Interference in protein Raman spectrum by fluorescence emission and signal–to–noise effect. Fluorescence emission can have severe destructive effects on the protein Raman spectrum. Intrinsic fluorescence usually occurs in the presence of aromatic amino acids, which can be eliminated by choosing the appropriate excitation wavelength in protein Raman studies. Also, transient fluorescence is usually due to impurity; a solvent or buffer is created to avoid interference. Transient fluorescence is necessary for Raman studies. Samples can be prepared as pure as possible. Background fluorescence was reduced by quenching or bleaching by emission light. Of course, it should be noted that increasing the temperature, in this case, may damage the sample (Tables 1–5).

Conclusion

High signal–to–noise ratio in the presence of a higher signal–to–noise ratio, the Raman spectrum of the sample is more accurate. This ratio can be increased by increasing the number of scans or the scan time.In addition, it should be noted that an excessive increase in the number of scans, as well as a change in the time interval of the scan, can cause serious damage to the sample. This method has many applications in various research fields. Also, this method provides important information about the structure of molecules, so that Raman bands can be considered as a kind of fingerprint of a compound. The similarities and differences between the Raman light scattering method and

the infrared absorption spectrometry method have made these two methods to be used for a more detailed structural study of a compound and complement each other. Raman spectroscopy provides valuable information on secondary, tertiary, and even quaternary structures of proteins. With the help of this method, it is possible to check the correct formation of disulfide bonds in the protein structure. Also, the amount of information that can be obtained from the protein Raman spectrum is far more than other conventional spectroscopic methods. Therefore, Raman spectroscopy is suggested as a useful tool to study the protein structure more precisely.

Acknowledgement

This study was supported by the Cancer Research Institute (CRI) Project of Scientific Instrument and Equipment Development, the National Natural Science Foundation of the United Sates, the International Joint BioSpectroscopy Core Research Laboratory (BCRL) Program supported by the California South University (CSU), and the Key project supported by the American International Standards Institute (AISI), Irvine, California, USA.

Table 1.

Role and applications of Raman spectroscopy and techniques in diagnosis of different types of human cancers.

Cancer Type	Technique	Raman Excitation Wavelength (nm)	Spot Size (mm)	Power (mW)	Signal Integration Time (s)	Number of Skin Lesions Studied and/or Patients	Reference
MM, BCC, SCC, actinic keratosis (AK), atypical nevi, melanocytic nevi, blue nevi, and seborrheic keratoses (SK)	Raman	785	3.5	300	1	518 (453 patients)	36
BCC, inflammatory scar tissues	Raman + OCT	785	0.044	40	30	1 patient	15
MM, BCC, SCC, pigmented nevi	Raman	785	1	150	30	50	37
MM, BCC, SCC, pigmented nevi	Raman + OCT	785	1	150	30	23, 50	38, 39
MM, BCC, SCC, pigmented nevi	Raman	785	0.1	17	10	137	40, 41
BCC, SCC, inflammatory scar tissues	Raman	825	0.005	40	30	21 (19 patients)	42
BCC	Raman	830	1.6	10	30	10 patients	43
BCC, SCC	Raman	830	–	200	20 (2 s×10 spectra)	31 (17 patients)	44
BCC, SCC, AK	Raman	830	0.17	200	20 (2 s×10 spectra)	49 (25 patients)	45
MM, BCC, SCC, actinic keratosis (AK), and non–melanoma pigmented lesions	Raman	830	0.2	100	1	137 (76 patients)	46, 47
BCC	Multi Modal	830	0.2	56	4	1 (healthy)	48
MM, eczema, psoriatic skin, malignant Kaposi sarcomas	Raman	1064	10	–	–	1 (healthy)	31
MM, BCC, pigmented nevi	Raman	1064	0.1	120	480	81 (72 patients)	49
Carotenoid concentration in BCC and actinic keratosis (AK)	Raman	488	2	10	20	14 patients	50
MM	Multi Modal	1064	0.08	–	35	Mice injected with human MM cells	51

Table 2.

Leading–edge portable biosensors and biomarkers data for Raman spectroscopy and imaging in cancer diagnosis.

	Subjects					Location			
Final lesion diagnosis	Mean age, year (range)	Male	Female	Number of lesions	Number biopsied (%)	Head and neck	Trunk	Upper limb	Lower limb
MM									
LM	69 (51–88)	12	8	20	20 (100)	19	1	0	0
LMM	67 (42–85)	7	1	8	8 (100)	8	0	0	0
SS	60 (22–77)	6	8	14	14 (100)	3	3	7	1
MM other	61 (60–62)	2	0	2	2 (100)	1	1	0	0
BCC									
Superficial	63 (34–86)	10	13	28	28 (100)	10	9	5	4
Nodular	66 (39–94)	34	29	73	73 (100)	52	10	9	2
Pigmented	67 (46–83)	2	4	6	6 (100)	2	4	0	0
Other BCC	68 (60–75)	1	1	2	2 (100)	1	1	0	0
SCC									
In situ	70 (56–88)	12	5	18	18 (100)	7	4	5	2
Invasive	66 (39–94)	16	10	28	28 (100)	16	1	5	6
Other SCC	78	0	1	1	1 (100)	1	0	0	0
Actinic keratosis (AK)	66 (43–92)	13	14	32	10 (31.3)	28	0	3	1
Atypical nevus	48 (20–75)	22	26	57	24 (42.1)	3	39	8	7
Junctional nevus	43 (18–70)	12	17	34	4 (11.8)	5	11	15	3
Compound nevus	35 (18–67)	13	15	30	6 (20)	9	8	9	4
Intradermal nevus	50 (28–83)	9	26	38	12 (31.6)	21	8	7	2
Blue nevus	37 (18–66)	4	9	13	4 (30.8)	4	1	6	2
Seborrheic keratosis (SK)	64 (25–89)	49	42	114	31 (27.2)	47	47	14	6
MM, malignant melanoma; MM subtypes: LM, lentigo maligna; LMM, lentigo maligna melanoma; SS, superficial spreading melanoma.									

Table 3.

Comparison between Mid–FTIR spectroscopy and Raman spectroscopy in cancer diagnosis.

	Mid–FTIR	Raman
Diagnostic criteria	Objective (based on biochemical spectral fingerprint)	
Wavenumber range	800–4000 cm^{-1}	400–4000 cm^{-1}
Type of spectroscopic detection	Mid–infrared light absorption using a polychromic light source	Inelastic light scattering using a monochromatic laser excitation (usually 785 or 830 nm but visible lasers also used)
Conditions for Raman/FTIR activation (selection rules)	Changes in the dipole moment	Changes in polarizability
Molecular bond sensitivities	Strong polar bonds including hydroxyl (OH), carbonyl (CO) and amide bonds	Non–polar bonds including C–C double and triple bonds including aromatic rings
SNR	Generally higher SNR in similar timescales	Weaker Raman cross–section of biological material results in lower SNR for normal Raman spectra
Spatial resolution	Lower spatial resolution due to diffraction limit (~ 10 μm). Synchrotron sources (2–5 μm)	Higher spatial resolution (~ 1 μm) due to diffraction limit
Imaging/mapping modes	Rapid scan imaging using focal plane or linear array detectors. ATR imaging can improve spatial resolutions and be applied to thicker samples	Point raster mapping, line and rapid synchronous readout mapping, Fast Raman imaging, ultrafast confocal Raman imaging, Wide–field imaging, LCTF Raman imaging
Enhanced techniques	ATR (attenuated total reflection): IR direct sample analysis by contact with an ATR crystal. Penetration is within the evanescent field which can be controlled and allows measurement from aqueous body fluids or non–dried tissue samples	SORS: the Raman scatter is collected from regions laterally offset from laser excitation, leading to significantly lower contributions from the surface layer, enabling depth probing. CARS: two laser beams are used to generate a coherent anti–Stokes frequency beam, which can be enhanced by resonance. SERS: enhancements over normal Raman scattering of typically 10^3–10^6 due to electromagnetic and chemical enhancement effects, with florescence quenching. Requires close proximity/adsorption onto a roughened metal surface, a colloidal solution or a roughened electrode (usually Ag or Au). Can tune to a specific chromophore for additional resonance enhancement (SERRS). TERS: combines high spatial resolution of an AFM and biochemical specificity of NRS
Sample preparation	Optimal thickness (transmission mode) or sample contact (ATR) may be necessary. Sample preparation is difficult	Little contact and destruction, water does not disturb measurement. Sample preparation is easier
Substrates	Mirror, CaF_2, BaF, Low e, zinc selenide (ZnSe)	CaF_2, BaF, quartz
Water	Strong water absorption and CO_2 contribution to spectrum	In vivo application possible due to weak scattering of water
Effect of paraffin–routine processing of tissue in histology	Paraffin peaks are visible in the FTIR fingerprint region. This can be overcome by deparaffinization or spectral subtraction	Strong Raman peaks in fingerprint region
Sample thickness	Spectra from thick samples (>15 μm) can cause spectral saturation	Point spectra can be obtained from thick sections (>15 μm) or bulk samples. 10–20 μm sections for mapping

Table 4.

Cancer type of interest and classification analysis groups of type of Raman system in cancer diagnosis.

Cancer type of interest	Classification analysis groups	Type of Raman system (HF/LF)	Authors (year)	Number of spectra (number of patients)	Analysis method Sensitivity: specificity	Reference
Skin cancer	Malignant + premalignant vs. benign and normal	Macro–Raman (LF)	Zeng group (2001–2012)	518 (453)	PCA–GDA and PLS 90%: 66%	20, 40–43
Skin cancer	Nonmelanoma cancers vs. normal lesions	Macro–Raman (LF)	Mahadevan–Jansen group (2008)	42 (19)	MRDF–SMLR 100%: 91%	44
Lung cancer	Malignant + premalignant vs. benign and normal	Macro–Raman (LF)	Zeng group (2008–2011)	129 (26)	PCA–LDA 90%: 91%	21, 47
Breast cancer	Tumor vs. normal (tumor tissue margin detection)	Macro–Raman (LF)	Feld group (2006)	30 (9)	Model fitting 100%: 100%	49
Colorectal cancer	Adenomatous tissue vs. hyperplastic polyps	Macro–Raman (LF)	Wilson group (2003)	19 (3)	PCA–LDA 100%: 89%	55

Table 4 (continued).
Cancer type of interest and classification analysis groups of type of Raman system in cancer diagnosis.

Cancer type of interest	Classification analysis groups	Type of Raman system (HF/LF)	Authors (year)	Number of spectra (number of patients)	Analysis method Sensitivity: specificity	Reference
Cervical cancer	Squamous dysplasia vs. normal, inflammation and metaplasia	Macro–Raman (LF)	Richards–Kortum group (2001)	27 (13)	Intensity ratios NA	63
Cervical cancer	High–grade preneoplastic lesions vs. normal	Macro–Raman (LF)	Mahadevan–Jansen group (2007)	172 (66)	Logistic regression 89%:>81%	64
Cervical cancer	1. Dysplasia vs. normal 2. High–grade dysplasia vs. normal 3. High–grade dysplasia vs normal	Macro–Raman (LF)	Huang group 1. (2009) 2. (2011) 3. (2012)	1. 92 (46) 2. 105 (29) 3. 476 (44)	PCA–LDA 1. 94%: 98% 2. 73%: 89% 3. 85%: 82%	65–67
Upper GI (esophageal cancer)	High–grade dysplasia vs. normal	Macro–Raman (LF)	Huang group (2013)	(2)	PLS–LDA 91%: 83%	71
Upper GI (stomach cancer)	1. Normal tissue 2. Benign ulcer 3. Malignant ulcer	Macro–Raman (LF)	Huang group 1. (2009) 2. (2010) 3. (2012)	65	PLS–LDA 1. 90.8%: 93.8% 2. 84.7%: 94.5% 3. 82.1%: 95.3%	68–70
Oral cavity	1. Normal vs. malignant 2. Normal vs. potentially malignant 3. Normal vs. diseased	Macro–Raman (LF)	Gupta group (2013)	802 (28 healthy + 171 nonhealthy)	MRDF–SMLR 1. 96%: 99% 2. 99%: 98% 3. 94%: 94%	72
Oral cavity	Premalignant and malignant vs. normal and benign	Macro–Raman (LF)	Sonis and Zeng group (2014)	(18)	PCA–LDA 100%: 77%	73, 74
Brain cancer	Normal brain vs. dense cancer and normal brain invaded by cancer cells	Macro–Raman (LF)	Leblond group (2015)	161 (17)	Boosted trees Machine learning 93%: 91%	77
Bladder cancer	Normal bladder vs. cancer	Macro–Raman (LF)	Bosch group (2010)	63	PCA–LDA 85%: 79%	80

Table 5.
Raman spectroscopy application, experimental set up and analysis method in cancer diagnosis.

Raman application		Experimental setup				Analysis method	Reference
		Wavelength (nm)	Power (mW)	Exposure time (sec)	Other		
Cancer detection	Breast cancer	830	100–150	10–30		Nonnegative least square (NNLS)	8
		830	82–125	1	Probe	NNLS	31
		786	N/A	4		Raman shifts	7
		830	65	10		PCA–LDA	34
		514.5	8	N/A		Hierarchical cluster	42
	Cervical cancer	785	80	5–15	Probe	Logistic regression	45
		785	80	5	Probe	Maximum representation and discrimination feature (MRDF)	47
						Sparse multinomial logistic regression (SMLR)	
		785	15	60	Probe	PCA–LDA	49
		785	10	60		Raman shifts	43
		785	100	30		PCA	50
	Colorectal cancer	785	300	5	Probe	PCA–Support vector machines (SVMs)	51
		785	70	N/A		PCA	35
						Hierarchical cluster	
						Multiple least squares (MLS)	
		782.5	11.5	60	LTRS	PCA– Logistic regression	52
		782.5	11.5	60	LTRS	PCA–Artificial neural network (ANN)	53
Allograft rejection	Cardiac rejection	785	100	10		PCA	54
	Renal rejection	785/514.5	8–12	10		PCA–Discriminant function analysis (DFA)	56

Table 5 (continued).

Raman spectroscopy application, experimental set up and analysis method in cancer diagnosis.

Raman application		Experimental setup				Analysis method	Reference
		Wavelength (nm)	Power (mW)	Exposure time (sec)	Other		
	Renal rejection	785/514.5	8–12	10		PCA–Discriminant function analysis (DFA)	56
SERS for biomarker		785	100	20		NNLS	65
		785	25	10		Raman shifts	66
		633	N/A	N/A		Raman shifts	9
SERS for in vivo		785	50	120		Partial least squares	75
		785	20	2		Raman shifts	10
SWNTs		N/A	100	2		Raman imaging using G–band	88
		785	100	3/10		Raman imaging using G–band	91
		785	80	0.5		Raman imaging using G–band	94
SERS imaging		785	60	N/A		Raman imaging using SERS peaks	100
		633	N/A	N/A		Raman imaging using SERS peaks	101
Core–shell nanoparticle		633	0.5/4	30/60		Raman shifts	105
		633	2	50		Raman shifts	109
		633	0.3	10		Raman shifts	110

References

1. Heidari A. Different High–Resolution Simulations of Medical, Medicinal, Clinical, Pharmaceutical and Therapeutics Oncology of Human Lung Cancer Translational Anti–Cancer Nano Drugs Delivery Treatment Process under Synchrotron and X–Ray Radiations. J Med Oncol. 2017;1(1):1.
2. Heidari A. A Modern Ethnomedicinal Technique for Transformation, Prevention and Treatment of Human Malignant Gliomas Tumors into Human Benign Gliomas Tumors under Synchrotron Radiation. Am J Ethnomed. 2017;4(1):10.
3. Heidari A. Active Targeted Nanoparticles for Anti–Cancer Nano Drugs Delivery across the Blood–Brain Barrier for Human Brain Cancer Treatment, Multiple Sclerosis (MS) and Alzheimer's Diseases Using Chemical Modifications of Anti–Cancer Nano Drugs or Drug–Nanoparticles through Zika Virus (ZIKV) Nanocarriers under Synchrotron Radiation. J Med Chem Toxicol. 2017;2(3):1–5.
4. Heidari A. Investigation of Medical, Medicinal, Clinical and Pharmaceutical Applications of Estradiol, Mestranol (Norlutin), Norethindrone (NET), Norethisterone Acetate (NETA), Norethisterone Enanthate (NETE) and Testosterone Nanoparticles as Biological Imaging, Cell Labeling, Anti–Microbial Agents and Anti–Cancer Nano Drugs in Nanomedicines Based Drug Delivery Systems for Anti–Cancer Targeting and Treatment. Parana Journal of Science and Education (PJSE). October 12, 2017;3(4):10-19.
5. Heidari A. A Comparative Computational and Experimental Study on Different Vibrational Biospectroscopy Methods, Techniques and Applications for Human Cancer Cells in Tumor Tissues Simulation, Modeling, Research, Diagnosis and Treatment. Open J Anal Bioanal Chem. 2017;1 (1): 014–020.
6. Heidari A. Combination of DNA/RNA Ligands and Linear/Non–Linear Visible–Synchrotron Radiation–Driven N–Doped Ordered Mesoporous Cadmium Oxide (CdO) Nanoparticles Photocatalysts Channels Resulted in an Interesting Synergistic Effect Enhancing Catalytic Anti–Cancer Activity. Enz Eng. 2017;6:1.
7. Heidari A. Modern Approaches in Designing Ferritin, Ferritin Light Chain, Transferrin, Beta–2 Transferrin and Bacterioferritin–Based Anti–Cancer Nano Drugs Encapsulating Nanosphere as DNA–Binding Proteins from Starved Cells (DPS). Mod Appro Drug Des. 2017;1(1). MADD.000504.
8. Heidari A. Potency of Human Interferon β–1a and Human Interferon β–1b in Enzymotherapy, Immunotherapy, Chemotherapy, Radiotherapy, Hormone Therapy and Targeted Therapy of Encephalomyelitis Disseminate/Multiple Sclerosis (MS) and Hepatitis A, B, C, D, E, F and G Virus Enter and Targets Liver Cells. J Proteomics Enzymol. 2017;6:1.
9. Heidari A. Transport Therapeutic Active Targeting of Human Brain Tumors Enable Anti–Cancer Nanodrugs Delivery across the Blood–Brain Barrier (BBB) to Treat Brain Diseases Using Nanoparticles and Nanocarriers under Synchrotron Radiation. J Pharm Pharmaceutics. 2017;4(2):1–5.
10. Heidari A. C. Brown, Combinatorial Therapeutic Approaches to DNA/RNA and Benzylpenicillin (Penicillin G), Fluoxetine Hydrochloride (Prozac and Sarafem), Propofol (Diprivan), Acetylsalicylic Acid (ASA) (Aspirin), Naproxen Sodium (Aleve and Naprosyn) and Dextromethamphetamine Nanocapsules with Surface Conjugated DNA/RNA to Targeted Nano Drugs for Enhanced Anti–Cancer Efficacy and Targeted Cancer Therapy Using Nano Drugs Delivery Systems. Ann Adv Chem. 2017;1(2):061–069.
11. Heidari A. High–Resolution Simulations of Human Brain Cancer Translational Nano Drugs Delivery Treatment Process under Synchrotron Radiation. J Transl Res. 2017;1(1):1–3.
12. Heidari A. Investigation of Anti–Cancer Nano Drugs' Effects' Trend on Human Pancreas Cancer Cells and Tissues Prevention, Diagnosis and Treatment Process under Synchrotron and X–Ray Radiations with the Passage of Time Using Mathematica. Current Trends Anal Bioanal Chem. 2017;1(1):36–41.
13. Heidari A. Pros and Cons Controversy on Molecular Imaging and Dynamics of Double–Standard DNA/RNA of Human Preserving Stem Cells–Binding Nano Molecules with Androgens/Anabolic Steroids (AAS) or Testosterone Derivatives through Tracking of Helium–4 Nucleus (Alpha

Particle) Using Synchrotron Radiation. Arch Biotechnol Biomed. 2017;1(1): 067–0100.
14. Heidari A. Visualizing Metabolic Changes in Probing Human Cancer Cells and Tissues Metabolism Using Vivo ^{1}H or Proton NMR, ^{13}C NMR, ^{15}N NMR and ^{31}P NMR Spectroscopy and Self–Organizing Maps under Synchrotron Radiation. SOJ Mater Sci Eng. 2017;5(2):1–6.
15. Heidari A. Cavity Ring–Down Spectroscopy (CRDS), Circular Dichroism Spectroscopy, Cold Vapour Atomic Fluorescence Spectroscopy and Correlation Spectroscopy Comparative Study on Malignant and Benign Human Cancer Cells and Tissues with the Passage of Time under Synchrotron Radiation. Enliven: Challenges Cancer Detect Ther. 2017;4(2):e001.
16. Heidari A. Laser Spectroscopy, Laser–Induced Breakdown Spectroscopy and Laser–Induced Plasma Spectroscopy Comparative Study on Malignant and Benign Human Cancer Cells and Tissues with the Passage of Time under Synchrotron Radiation. Int J Hepatol Gastroenterol. 2017;3(4):079–084.
17. Heidari A. Time–Resolved Spectroscopy and Time–Stretch Spectroscopy Comparative Study on Malignant and Benign Human Cancer Cells and Tissues with the Passage of Time under Synchrotron Radiation. Enliven: Pharmacovigilance and Drug Safety.2017;4(2):e001.
18. Heidari A. Overview of the Role of Vitamins in Reducing Negative Effect of Decapeptyl (Triptorelin Acetate or Pamoate Salts) on Prostate Cancer Cells and Tissues in Prostate Cancer Treatment Process through Transformation of Malignant Prostate Tumors into Benign Prostate Tumors under Synchrotron Radiation. Open J Anal Bioanal Chem. 2017;1(1):021–026.
19. Heidari A. Electron Phenomenological Spectroscopy, Electron Paramagnetic Resonance (EPR) Spectroscopy and Electron Spin Resonance (ESR) Spectroscopy Comparative Study on Malignant and Benign Human Cancer Cells and Tissues with the Passage of Time under Synchrotron Radiation. Austin J Anal Pharm Chem. 2017;4(3):1091.
20. Heidari A. Therapeutic Nanomedicine Different High–Resolution Experimental Images and Computational Simulations for Human Brain Cancer Cells and Tissues Using Nanocarriers Deliver DNA/RNA to Brain Tumors under Synchrotron Radiation with the Passage of Time Using Mathematica and MATLAB. Madridge J Nano Tech. Sci. 2017;2(2):77–83.
21. Heidari A. A Consensus and Prospective Study on Restoring Cadmium Oxide (CdO) Nanoparticles Sensitivity in Recurrent Ovarian Cancer by Extending the Cadmium Oxide (CdO) Nanoparticles–Free Interval Using Synchrotron Radiation Therapy as Antibody–Drug Conjugate for the Treatment of Limited–Stage Small Cell Diverse Epithelial Cancers. Cancer Clin Res Rep. 2017;1:2, e001.
22. Heidari A. A Novel and Modern Experimental Imaging and Spectroscopy Comparative Study on Malignant and Benign Human Cancer Cells and Tissues with the Passage of Time under White Synchrotron Radiation. Cancer Sci Res Open Access. 2017;4(2):1–8.
23. Heidari A. Different High–Resolution Simulations of Medical, Medicinal, Clinical, Pharmaceutical and Therapeutics Oncology of Human Breast Cancer Translational Nano Drugs Delivery Treatment Process under Synchrotron and X–Ray Radiations. J Oral Cancer Res. 2017;1(1):12–17.
24. Heidari A. Vibrational Decihertz (dHz), Centihertz (cHz), Millihertz (mHz), Microhertz (μHz), Nanohertz (nHz), Picohertz (pHz), Femtohertz (fHz), Attohertz (aHz), Zeptohertz (zHz) and Yoctohertz (yHz) Imaging and Spectroscopy Comparative Study on Malignant and Benign Human Cancer Cells and Tissues under Synchrotron Radiation. International Journal of Biomedicine. 2017;7(4):335–340.
25. Heidari A. Force Spectroscopy and Fluorescence Spectroscopy Comparative Study on Malignant and Benign Human Cancer Cells and Tissues with the Passage of Time under Synchrotron Radiation. EC Cancer. 2017;2(5):239–246.
26. Heidari A. Photoacoustic Spectroscopy, Photoemission Spectroscopy and Photothermal Spectroscopy Comparative Study on Malignant and Benign Human Cancer Cells and Tissues with the Passage of Time under Synchrotron Radiation. BAOJ Cancer Res Ther. 2017;3(3): 045–052.
27. Heidari A. J–Spectroscopy, Exchange Spectroscopy (EXSY), Nuclear Overhauser Effect Spectroscopy (NOESY) and Total Correlation Spectroscopy (TOCSY) Comparative Study on Malignant and Benign Human Cancer Cells and Tissues under Synchrotron Radiation. EMS Eng Sci J. 2017;1(2):006–013.
28. Heidari A. Neutron Spin Echo Spectroscopy and Spin Noise Spectroscopy Comparative Study on Malignant and Benign Human Cancer Cells and Tissues with the Passage of Time under Synchrotron Radiation. Int J Biopharm Sci. 2017;1:103–107.
29. Heidari A. Vibrational Decahertz (daHz), Hectohertz (hHz), Kilohertz (kHz), Megahertz (MHz), Gigahertz (GHz), Terahertz (THz), Petahertz (PHz), Exahertz (EHz), Zettahertz (ZHz) and Yottahertz (YHz) Imaging and Spectroscopy Comparative Study on Malignant and Benign Human Cancer Cells and Tissues under Synchrotron Radiation. Madridge J Anal Sci Instrum, 2017;2(1):41–46.
30. Heidari A. Two–Dimensional Infrared Correlation Spectroscopy, Linear Two–Dimensional Infrared Spectroscopy and Non–Linear Two–Dimensional Infrared Spectroscopy Comparative Study on Malignant and Benign Human Cancer Cells and Tissues under Synchrotron Radiation with the Passage of Time. J Mater Sci Nanotechnol. 2018;6(1):101.
31. Heidari A. Fourier Transform Infrared (FTIR) Spectroscopy, Near–Infrared Spectroscopy (NIRS) and Mid–Infrared Spectroscopy (MIRS) Comparative Study on Malignant and Benign Human Cancer Cells and Tissues under Synchrotron Radiation with the Passage of Time. Int J Nanotechnol Nanomed. 2018;3(1):1–6.
32. Heidari A. Infrared Photo Dissociation Spectroscopy and Infrared Correlation Table Spectroscopy Comparative Study on Malignant and Benign Human Cancer Cells and Tissues under Synchrotron Radiation with the Passage of Time. Austin Pharmacol Pharm. 2018;3(1): 1011.
33. Heidari A. Novel and Transcendental Prevention, Diagnosis and Treatment Strategies for Investigation of Interaction among Human Blood Cancer Cells, Tissues, Tumors and Metastases with Synchrotron Radiation under Anti–Cancer Nano Drugs Delivery Efficacy Using MATLAB Modeling and Simulation. Madridge J Nov Drug Res. 2017;1(1):18–24.
34. Heidari A. Comparative Study on Malignant and Benign Human Cancer Cells and Tissues with the Passage of Time under Synchrotron Radiation. Open Access J Trans Med Res. 2018;2 (1):00026–00032.
35. Gobato MRR, Gobato R, Heidari A. Planting of Jaboticaba Trees for Landscape Repair of Degraded Area. Landscape Architecture and Regional Planning. 2018;3(1)1–9.
36. Heidari A. Fluorescence Spectroscopy, Phosphorescence Spectroscopy and Luminescence Spectroscopy Comparative

Study on Malignant and Benign Human Cancer Cells and Tissues under Synchrotron Radiation with the Passage of Time. SM J Clin. Med. Imaging. 2018;4(1): 1018.
37. Heidari A. Nuclear Inelastic Scattering Spectroscopy (NISS) and Nuclear Inelastic Absorption Spectroscopy (NIAS) Comparative Study on Malignant and Benign Human Cancer Cells and Tissues under Synchrotron Radiation. Int J Pharm Sci. 2018;2(1):1–14.
38. Heidari A. X–Ray Diffraction (XRD), Powder X–Ray Diffraction (PXRD) and Energy–Dispersive X–Ray Diffraction (EDXRD) Comparative Study on Malignant and Benign Human Cancer Cells and Tissues under Synchrotron Radiation. J Oncol Res. 2018;2(1):1–14.
39. Heidari A. Correlation Two–Dimensional Nuclear Magnetic Resonance (NMR) (2D–NMR) (COSY) Imaging and Spectroscopy Comparative Study on Malignant and Benign Human Cancer Cells and Tissues under Synchrotron Radiation. EMS Can Sci, 1–1–001, 2018.
40. Heidari A. Thermal Spectroscopy, Photothermal Spectroscopy, Thermal Microspectroscopy, Photothermal Microspectroscopy, Thermal Macrospectroscopy and Photothermal Macrospectroscopy Comparative Study on Malignant and Benign Human Cancer Cells and Tissues with the Passage of Time under Synchrotron Radiation. SM J Biometrics Biostat. 2018;3(1):1024.
41. Heidari A. A Modern and Comprehensive Experimental Biospectroscopic Comparative Study on Human Common Cancers' Cells, Tissues and Tumors before and after Synchrotron Radiation Therapy. Open Acc J Oncol Med. 2018;1(1).
42. Heidari A. Heteronuclear Correlation Experiments Such as Heteronuclear Single–Quantum Correlation Spectroscopy (HSQC), Heteronuclear Multiple–Quantum Correlation Spectroscopy (HMQC) and Heteronuclear Multiple–Bond Correlation Spectroscopy (HMBC) Comparative Study on Malignant and Benign Human Endocrinology and Thyroid Cancer Cells and Tissues under Synchrotron Radiation. J Endocrinol Thyroid Res. 2018;3(1):555603.
43. Heidari A. Nuclear Resonance Vibrational Spectroscopy (NRVS), Nuclear Inelastic Scattering Spectroscopy (NISS), Nuclear Inelastic Absorption Spectroscopy (NIAS) and Nuclear Resonant Inelastic X–Ray Scattering Spectroscopy (NRIXSS) Comparative Study on Malignant and Benign Human Cancer Cells and Tissues under Synchrotron Radiation. Int J Bioorg Chem Mol Biol. 2018;6(1e):1–5.
44. Heidari A. A Novel and Modern Experimental Approach to Vibrational Circular Dichroism Spectroscopy and Video Spectroscopy Comparative Study on Malignant and Benign Human Cancer Cells and Tissues with the Passage of Time under White and Monochromatic Synchrotron Radiation. Glob J Endocrinol Metab. 2018;1(3). GJEM. 000514–000519.
45. Heidari A. Pros and Cons Controversy on Heteronuclear Correlation Experiments Such as Heteronuclear Single–Quantum Correlation Spectroscopy (HSQC), Heteronuclear Multiple–Quantum Correlation Spectroscopy (HMQC) and Heteronuclear Multiple–Bond Correlation Spectroscopy (HMBC) Comparative Study on Malignant and Benign Human Cancer Cells and Tissues under Synchrotron Radiation. EMS Pharma J. 2018;1(1):002–008.
46. Heidari A. A Modern Comparative and Comprehensive Experimental Biospectroscopic Study on Different Types of Infrared Spectroscopy of Malignant and Benign Human Cancer Cells and Tissues with the Passage of Time under Synchrotron Radiation. J Analyt Molecul Tech. 2018;3(1):8.
47. Heidari A. Investigation of Cancer Types Using Synchrotron Technology for Proton Beam Therapy: An Experimental Biospectroscopic Comparative Study. European Modern Studies Journal. 2018;2(1):13–29.
48. Heidari A. Saturated Spectroscopy and Unsaturated Spectroscopy Comparative Study on Malignant and Benign Human Cancer Cells and Tissues with the Passage of Time under Synchrotron Radiation. Imaging J Clin Medical Sci. 2018;5(1):001–007.
49. Heidari A. Small–Angle Neutron Scattering (SANS) and Wide–Angle X–Ray Diffraction (WAXD) Comparative Study on Malignant and Benign Human Cancer Cells and Tissues under Synchrotron Radiation. Int J Bioorg Chem Mol Biol. 2018;6(2e):1–6.
50. Heidari A. Investigation of Bladder Cancer, Breast Cancer, Colorectal Cancer, Endometrial Cancer, Kidney Cancer, Leukemia, Liver, Lung Cancer, Melanoma, Non–Hodgkin Lymphoma, Pancreatic Cancer, Prostate Cancer, Thyroid Cancer and Non–Melanoma Skin Cancer Using Synchrotron Technology for Proton Beam Therapy: An Experimental Biospectroscopic Comparative Study. Ther Res Skin Dis. 2018;1(1).
51. Heidari A. Attenuated Total Reflectance Fourier Transform Infrared (ATR–FTIR) Spectroscopy, Micro–Attenuated Total Reflectance Fourier Transform Infrared (Micro–ATR–FTIR) Spectroscopy and Macro–Attenuated Total Reflectance Fourier Transform Infrared (Macro–ATR–FTIR) Spectroscopy Comparative Study on Malignant and Benign Human Cancer Cells and Tissues under Synchrotron Radiation with the Passage of Time. International Journal of Chemistry Papers. 2018;2(1):1–12.
52. Heidari A. Mössbauer Spectroscopy, Mössbauer Emission Spectroscopy and ^{57}Fe Mössbauer Spectroscopy Comparative Study on Malignant and Benign Human Cancer Cells and Tissues under Synchrotron Radiation. Acta Scientific Cancer Biology 2.3: 17–20, 2018.
53. Heidari A. Comparative Study on Malignant and Benign Human Cancer Cells and Tissues under Synchrotron Radiation with the Passage of Time. Organic & Medicinal Chem IJ. 2018;6(1):555676.
54. Heidari A. Correlation Spectroscopy, Exclusive Correlation Spectroscopy and Total Correlation Spectroscopy Comparative Study on Malignant and Benign Human AIDS–Related Cancers Cells and Tissues with the Passage of Time under Synchrotron Radiation. Int J Bioanal Biomed. 2018;2(1):001–007.
55. Heidari A. Biomedical Instrumentation and Applications of Biospectroscopic Methods and Techniques in Malignant and Benign Human Cancer Cells and Tissues Studies under Synchrotron Radiation and Anti–Cancer Nano Drugs Delivery. Am J Nanotechnol Nanomed. 2018;1(1):001–009.
56. Heidari A. Vivo ^{1}H or Proton NMR, ^{13}C NMR, ^{15}N NMR and ^{31}P NMR Spectroscopy Comparative Study on Malignant and Benign Human Cancer Cells and Tissues under Synchrotron Radiation. Ann Biomet Biostat. 2018;1(1):1001.
57. Heidari A. Grazing–Incidence Small–Angle Neutron Scattering (GISANS) and Grazing–Incidence X–Ray Diffraction (GIXD) Comparative Study on Malignant and Benign Human Cancer Cells, Tissues and Tumors under Synchrotron Radiation. Ann Cardiovasc Surg. 2018;1 (2):1006.
58. Heidari A. Adsorption Isotherms and Kinetics of Multi–Walled Carbon Nanotubes (MWCNTs), Boron Nitride Nanotubes (BNNTs), Amorphous Boron Nitride Nanotubes (a–BNNTs) and Hexagonal Boron Nitride Nanotubes (h–BNNTs)

for Eliminating Carcinoma, Sarcoma, Lymphoma, Leukemia, Germ Cell Tumor and Blastoma Cancer Cells and Tissues. Clin Med Rev Case Rep. 2018;5:201.
59. Heidari A. Correlation Spectroscopy (COSY), Exclusive Correlation Spectroscopy (ECOSY), Total Correlation Spectroscopy (TOCSY), Incredible Natural–Abundance Double–Quantum Transfer Experiment (INADEQUATE), Heteronuclear Single–Quantum Correlation Spectroscopy (HSQC), Heteronuclear Multiple–Bond Correlation Spectroscopy (HMBC), Nuclear Overhauser Effect Spectroscopy (NOESY) and Rotating Frame Nuclear Overhauser Effect Spectroscopy (ROESY) Comparative Study on Malignant and Benign Human Cancer Cells and Tissues under Synchrotron Radiation. Acta Scientific Pharmaceutical Sciences. 2018;2(5):30–35.
60. Heidari A. Small–Angle X–Ray Scattering (SAXS), Ultra–Small Angle X–Ray Scattering (USAXS), Fluctuation X–Ray Scattering (FXS), Wide–Angle X–Ray Scattering (WAXS), Grazing–Incidence Small–Angle X–Ray Scattering (GISAXS), Grazing–Incidence Wide–Angle X–Ray Scattering (GIWAXS), Small–Angle Neutron Scattering (SANS), Grazing–Incidence Small–Angle Neutron Scattering (GISANS), X–Ray Diffraction (XRD), Powder X–Ray Diffraction (PXRD), Wide–Angle X–Ray Diffraction (WAXD), Grazing–Incidence X–Ray Diffraction (GIXD) and Energy–Dispersive X–Ray Diffraction (EDXRD) Comparative Study on Malignant and Benign Human Cancer Cells and Tissues under Synchrotron Radiation. Oncol Res Rev. 2018;1(1):1–10.
61. Heidari A. Pump–Probe Spectroscopy and Transient Grating Spectroscopy Comparative Study on Malignant and Benign Human Cancer Cells and Tissues with the Passage of Time under Synchrotron Radiation. Adv Material Sci Engg. 2018;2(1):1–7.
62. Heidari A. Grazing–Incidence Small–Angle X–Ray Scattering (GISAXS) and Grazing–Incidence Wide–Angle X–Ray Scattering (GIWAXS) Comparative Study on Malignant and Benign Human Cancer Cells and Tissues under Synchrotron Radiation. Insights Pharmacol Pharm Sci. 2018;1(1):1–8.
63. Heidari A. Acoustic Spectroscopy, Acoustic Resonance Spectroscopy and Auger Spectroscopy Comparative Study on Anti–Cancer Nano Drugs Delivery in Malignant and Benign Human Cancer Cells and Tissues with the Passage of Time under Synchrotron Radiation. Nanosci Technol. 2018;5(1):1–9.
64. Heidari A. Niobium, Technetium, Ruthenium, Rhodium, Hafnium, Rhenium, Osmium and Iridium Ions Incorporation into the Nano Polymeric Matrix (NPM) by Immersion of the Nano Polymeric Modified Electrode (NPME) as Molecular Enzymes and Drug Targets for Human Cancer Cells, Tissues and Tumors Treatment under Synchrotron and Synchrocyclotron Radiations. Nanomed Nanotechnol. 2018;3(2):000138.
65. Heidari A. Homonuclear Correlation Experiments Such as Homonuclear Single–Quantum Correlation Spectroscopy (HSQC), Homonuclear Multiple–Quantum Correlation Spectroscopy (HMQC) and Homonuclear Multiple–Bond Correlation Spectroscopy (HMBC) Comparative Study on Malignant and Benign Human Cancer Cells and Tissues under Synchrotron Radiation. Austin J Proteomics Bioinform & Genomics. 2018;5(1):1024.
66. Heidari A. Atomic Force Microscopy Based Infrared (AFM–IR) Spectroscopy and Nuclear Resonance Vibrational Spectroscopy Comparative Study on Malignant and Benign Human Cancer Cells and Tissues under Synchrotron Radiation with the Passage of Time. J Appl Biotechnol Bioeng. 2018;5(3):142–148.
67. Heidari A. Time–Dependent Vibrational Spectral Analysis of Malignant and Benign Human Cancer Cells and Tissues under Synchrotron Radiation. J Cancer Oncol, 2018;2(2): 000124.
68. Heidari A. Palauamine and Olympiadane Nano Molecules Incorporation into the Nano Polymeric Matrix (NPM) by Immersion of the Nano Polymeric Modified Electrode (NPME) as Molecular Enzymes and Drug Targets for Human Cancer Cells, Tissues and Tumors Treatment under Synchrotron and Synchrocyclotron Radiations. Arc Org Inorg Chem Sci. 2018;3(1).
69. Gobato R, Heidari A. Infrared Spectrum and Sites of Action of Sanguinarine by Molecular Mechanics and Ab Initio Methods. International Journal of Atmospheric and Oceanic Sciences. 2018;2(1):1–9.
70. Heidari A. Angelic Acid, Diabolic Acids, Draculin and Miraculin Nano Molecules Incorporation into the Nano Polymeric Matrix (NPM) by Immersion of the Nano Polymeric Modified Electrode (NPME) as Molecular Enzymes and Drug Targets for Human Cancer Cells, Tissues and Tumors Treatment under Synchrotron and Synchrocyclotron Radiations. Med & Analy Chem Int J. 2018;2(1):000111.
71. Heidari A. Gamma Linolenic Methyl Ester, 5–Heptadeca–5,8,11–Trienyl1,3,4–Oxadiazole–2–Thiol, Sulphoquinovosyl Diacyl Glycerol, Ruscogenin, Nocturnoside B, Protodioscine B, Parquisoside–B, Leiocarposide, Narangenin, 7–Methoxy Hespertin, Lupeol, Rosemariquinone, Rosmanol and Rosemadiol Nano Molecules Incorporation into the Nano Polymeric Matrix (NPM) by Immersion of the Nano Polymeric Modified Electrode (NPME) as Molecular Enzymes and Drug Targets for Human Cancer Cells, Tissues and Tumors Treatment under Synchrotron and Synchrocyclotron Radiations. Int J Pharma Anal Acta. 2018;2(1):007–014.
72. Heidari A. Fourier Transform Infrared (FTIR) Spectroscopy, Attenuated Total Reflectance Fourier Transform Infrared (ATR–FTIR) Spectroscopy, Micro–Attenuated Total Reflectance Fourier Transform Infrared (Micro–ATR–FTIR) Spectroscopy, Macro–Attenuated Total Reflectance Fourier Transform Infrared (Macro–ATR–FTIR) Spectroscopy, Two–Dimensional Infrared Correlation Spectroscopy, Linear Two–Dimensional Infrared Spectroscopy, Non–Linear Two–Dimensional Infrared Spectroscopy, Atomic Force Microscopy Based Infrared (AFM–IR) Spectroscopy, Infrared Photodissociation Spectroscopy, Infrared Correlation Table Spectroscopy, Near–Infrared Spectroscopy (NIRS), Mid–Infrared Spectroscopy (MIRS), Nuclear Resonance Vibrational Spectroscopy, Thermal Infrared Spectroscopy and Photothermal Infrared Spectroscopy Comparative Study on Malignant and Benign Human Cancer Cells and Tissues under Synchrotron Radiation with the Passage of Time. Glob Imaging Insights. 2018;3(2):1–14.
73. Heidari A. Heteronuclear Single–Quantum Correlation Spectroscopy (HSQC) and Heteronuclear Multiple–Bond Correlation Spectroscopy (HMBC) Comparative Study on Malignant and Benign Human Cancer Cells, Tissues and Tumors under Synchrotron and Synchrocyclotron Radiations. Chronicle of Medicine and Surgery. 2018;2(3):144–156.
74. Heidari A. Tetrakis [3, 5–bis (Trifluoromethyl) Phenyl] Borate (BARF)–Enhanced Precatalyst Preparation Stabilization and Initiation (EPPSI) Nano Molecules. Medical Research and Clinical Case Reports. 2018;2(1):113–126.
75. Heidari A. Sydnone, Münchnone, Montréalone, Mogone, Montelukast, Quebecol and Palau'amine–Enhanced Precatalyst Preparation Stabilization and Initiation (EPPSI) Nano

Molecules. Sur Cas Stud Op Acc J. 2018;1(3).
76. Heidari A. Fornacite, Orotic Acid, Rhamnetin, Sodium Ethyl Xanthate (SEX) and Spermine (Spermidine or Polyamine) Nanomolecules Incorporation into the Nanopolymeric Matrix (NPM). International Journal of Biochemistry and Biomolecules. 2018;4(1):1–19.
77. Heidari A. R. Gobato, Putrescine, Cadaverine, Spermine and Spermidine–Enhanced Precatalyst Preparation Stabilization and Initiation (EPPSI) Nano Molecules. Parana Journal of Science and Education (PJSE). July 1, 2018;4(5):1–14.
78. Heidari A. Cadaverine (1,5–Pentanediamine or Pentamethylenediamine), Diethyl Azodicarboxylate (DEAD or DEADCAT) and Putrescine (Tetramethylenediamine) Nano Molecules Incorporation into the Nano Polymeric Matrix (NPM) by Immersion of the Nano Polymeric Modified Electrode (NPME) as Molecular Enzymes and Drug Targets for Human Cancer Cells, Tissues and Tumors Treatment under Synchrotron and Synchrocyclotron Radiations. Hiv and Sexual Health Open Access Open Journal. 2018;1(1):4–11.
79. Heidari A. Improving the Performance of Nano–Endofullerenes in Polyaniline Nanostructure–Based Biosensors by Covering Californium Colloidal Nanoparticles with Multi–Walled Carbon Nanotubes. Journal of Advances in Nanomaterials. 2018;3(1):1–28.
80. Gobato R, Heidari A. Molecular Mechanics and Quantum Chemical Study on Sites of Action of Sanguinarine Using Vibrational Spectroscopy Based on Molecular Mechanics and Quantum Chemical Calculations. Malaysian Journal of Chemistry. 2018; 20 (1):1–23.
81. Heidari A. Vibrational Biospectroscopic Studies on Anti–Cancer Nanopharmaceuticals (Part I). Malaysian Journal of Chemistry. 2018;20 (1):33–73.
82. Heidari A. Vibrational Biospectroscopic Studies on Anti–Cancer Nanopharmaceuticals (Part II). Malaysian Journal of Chemistry. 2018;20 (1):74–117.
83. Heidari A. Uranocene ($U(C_8H_8)_2$) and Bis(Cyclooctatetraene) Iron ($Fe(C_8H_8)_2$ or $Fe(COT)_2$)–Enhanced Precatalyst Preparation Stabilization and Initiation (EPPSI) Nano Molecules. Chemistry Reports. 2018;1(2):1–16.
84. Heidari A. Biomedical Systematic and Emerging Technological Study on Human Malignant and Benign Cancer Cells and Tissues Biospectroscopic Analysis under Synchrotron Radiation. Glob Imaging Insights. 2018;3(3):1–7.
85. Heidari A. Deep–Level Transient Spectroscopy and X–Ray Photoelectron Spectroscopy (XPS) Comparative Study on Malignant and Benign Human Cancer Cells and Tissues with the Passage of Time under Synchrotron Radiation. Res Dev Material Sci. 2018;7(2). RDMS.000659,
86. Heidari A. C70–Carboxyfullerenes Nano Molecules Incorporation into the Nano Polymeric Matrix (NPM) by Immersion of the Nano Polymeric Modified Electrode (NPME) as Molecular Enzymes and Drug Targets for Human Cancer Cells, Tissues and Tumors Treatment under Synchrotron and Synchrocyclotron Radiations. Glob Imaging Insights. 2018;3(3):1–7.
87. Heidari A. The Effect of Temperature on Cadmium Oxide (CdO) Nanoparticles Produced by Synchrotron Radiation in the Human Cancer Cells, Tissues and Tumors. International Journal of Advanced Chemistry. 2018;6(2):140–156.
88. Heidari A. A Clinical and Molecular Pathology Investigation of Correlation Spectroscopy (COSY), Exclusive Correlation Spectroscopy (ECOSY), Total Correlation Spectroscopy (TOCSY), Heteronuclear Single–Quantum Correlation Spectroscopy (HSQC) and Heteronuclear Multiple–Bond Correlation Spectroscopy (HMBC) Comparative Study on Malignant and Benign Human Cancer Cells, Tissues and Tumors under Synchrotron and Synchrocyclotron Radiations Using Cyclotron versus Synchrotron, Synchrocyclotron and the Large Hadron Collider (LHC) for Delivery of Proton and Helium Ion (Charged Particle) Beams for Oncology Radiotherapy. European Journal of Advances in Engineering and Technology. 2018;5(7):414–426.
89. Heidari A. Nano Molecules Incorporation into the Nano Polymeric Matrix (NPM) by Immersion of the Nano Polymeric Modified Electrode (NPME) as Molecular Enzymes and Drug Targets for Human Cancer Cells, Tissues and Tumors Treatment under Synchrotron and Synchrocyclotron Radiations. J Oncol Res. 2018;1(1):1–20.
90. Heidari A. Use of Molecular Enzymes in the Treatment of Chronic Disorders. Canc Oncol Open Access J. 2018;1(1):12–15.
91. Heidari A. Vibrational Biospectroscopic Study and Chemical Structure Analysis of Unsaturated Polyamides Nanoparticles as Anti–Cancer Polymeric Nanomedicines Using Synchrotron Radiation. International Journal of Advanced Chemistry. 2018;6(2):167–189.
92. Heidari A. Adamantane, Irene, Naftazone and Pyridine–Enhanced Precatalyst Preparation Stabilization and Initiation (PEPPSI) Nano Molecules. Madridge J Nov Drug Res. 2018;2(1):61–67.
93. Heidari A. Heteronuclear Single–Quantum Correlation Spectroscopy (HSQC) and Heteronuclear Multiple–Bond Correlation Spectroscopy (HMBC) Comparative Study on Malignant and Benign Human Cancer Cells and Tissues with the Passage of Time under Synchrotron Radiation. Madridge J Nov Drug Res. 2018;2(1):68–74.
94. Heidari A. R. Gobato, A Novel Approach to Reduce Toxicities and to Improve Bioavailabilities of DNA/RNA of Human Cancer Cells–Containing Cocaine (Coke), Lysergide (Lysergic Acid Diethyl Amide or LSD), Δ^9–Tetrahydrocannabinol (THC) [(–)–trans–Δ^9–Tetrahydrocannabinol], Theobromine (Xantheose), Caffeine, Aspartame (APM) (NutraSweet) and Zidovudine (ZDV) Azidothymidine (AZT). as Anti–Cancer Nano Drugs by Coassembly of Dual Anti–Cancer Nano Drugs to Inhibit DNA/RNA of Human Cancer Cells Drug Resistance. Parana Journal of Science and Education (PJSE). 2018;4(6):1–17.
95. Heidari A, Gobato R. Ultraviolet Photoelectron Spectroscopy (UPS) and Ultraviolet–Visible (UV–Vis) Spectroscopy Comparative Study on Malignant and Benign Human Cancer Cells and Tissues with the Passage of Time under Synchrotron Radiation. Parana Journal of Science and Education (PJSE). 2018;4(6):18–33.
96. Gobato R, Heidari A, Mitra A. The Creation of $C_{13}H_{20}BeLi_2SeSi$. The Proposal of a Bio–Inorganic Molecule, Using Ab Initio Methods for the Genesis of a Nano Membrane. Arc Org Inorg Chem Sci. 2018;3(4) AOICS.MS.ID.000167.
97. Gobato R, Heidari A. Using the Quantum Chemistry for Genesis of a Nano Biomembrane with a Combination of the Elements Be, Li, Se, Si, C and H. J Nanomed Res. 2018;7(4):241–252.
98. Heidari A. Bastadins and Bastaranes–Enhanced Precatalyst Preparation Stabilization and Initiation (EPPSI) Nano Molecules. Glob Imaging Insights. 2018;3(4):1–7.
99. Heidari A. Fucitol, Pterodactyladiene, DEAD or DEADCAT (DiEthyl AzoDiCArboxylaTe), Skatole, the NanoPutians, Thebacon, Pikachurin, Tie Fighter, Spermidine and Mirasorvone Nano Molecules Incorporation into the Nano

Polymeric Matrix (NPM) by Immersion of the Nano Polymeric Modified Electrode (NPME) as Molecular Enzymes and Drug Targets for Human Cancer Cells, Tissues and Tumors Treatment under Synchrotron and Synchrocyclotron Radiations. Glob Imaging Insights. 2018;3(4):1–8.
100. Dadvar E, Heidari A. A Review on Separation Techniques of Graphene Oxide (GO)/Base on Hybrid Polymer Membranes for Eradication of Dyes and Oil Compounds: Recent Progress in Graphene Oxide (GO)/Base on Polymer Membranes–Related Nanotechnologies. Clin Med Rev Case Rep. 2018;5:228.
101. Heidari A, Gobato R. First–Time Simulation of Deoxyuridine Monophosphate (dUMP) (Deoxyuridylic Acid or Deoxyuridylate) and Vomitoxin (Deoxynivalenol (DON)) ((3α,7α)–3,7,15–Trihydroxy–12,13–Epoxytrichothec–9–En–8–One)–Enhanced Precatalyst Preparation Stabilization and Initiation (EPPSI) Nano Molecules Incorporation into the Nano Polymeric Matrix (NPM) by Immersion of the Nano Polymeric Modified Electrode (NPME) as Molecular Enzymes and Drug Targets for Human Cancer Cells, Tissues and Tumors Treatment under Synchrotron and Synchrocyclotron Radiations. Parana Journal of Science and Education (PJSE). 2018;4(6):46–67.
102. Heidari A. Buckminsterfullerene (Fullerene), Bullvalene, Dickite and Josiphos Ligands Nano Molecules Incorporation into the Nano Polymeric Matrix (NPM) by Immersion of the Nano Polymeric Modified Electrode (NPME) as Molecular Enzymes and Drug Targets for Human Hematology and Thromboembolic Diseases Prevention, Diagnosis and Treatment under Synchrotron and Synchrocyclotron Radiations. Glob Imaging Insights. 2018;3(4):1–7.
103. Heidari A. Fluctuation X–Ray Scattering (FXS) and Wide–Angle X–Ray Scattering (WAXS) Comparative Study on Malignant and Benign Human Cancer Cells and Tissues under Synchrotron Radiation. Glob Imaging Insights. 2018;3(4):1–7.
104.Heidari A. A Novel Approach to Correlation Spectroscopy (COSY), Exclusive Correlation Spectroscopy (ECOSY), Total Correlation Spectroscopy (TOCSY), Incredible Natural–Abundance Double–Quantum Transfer Experiment (INADEQUATE), Heteronuclear Single–Quantum Correlation Spectroscopy (HSQC), Heteronuclear Multiple–Bond Correlation Spectroscopy (HMBC), Nuclear Overhauser Effect Spectroscopy (NOESY) and Rotating Frame Nuclear Overhauser Effect Spectroscopy (ROESY) Comparative Study on Malignant and Benign Human Cancer Cells and Tissues under Synchrotron Radiation. Glob Imaging Insights. 2018;3(5):1–9.
105.Heidari A. Terphenyl–Based Reversible Receptor with Rhodamine, Rhodamine–Based Molecular Probe, Rhodamine–Based Using the Spirolactam Ring Opening, Rhodamine B with Ferrocene Substituent, Calix4.Arene–Based Receptor, Thioether + Aniline–Derived Ligand Framework Linked to a Fluorescein Platform, Mercuryfluor–1 (Flourescent Probe), N,N'–Dibenzyl–1,4,10,13–Tetraraoxa–7,16–Diazacyclooctadecane and Terphenyl–Based Reversible Receptor with Pyrene and Quinoline as the Fluorophores–Enhanced Precatalyst Preparation Stabilization and Initiation (EPPSI) Nano Molecules. Glob Imaging Insights. 2018;3(5):1–9.
106. Heidari A. Small–Angle X–Ray Scattering (SAXS), Ultra–Small Angle X–Ray Scattering (USAXS), Fluctuation X–Ray Scattering (FXS), Wide–Angle X–Ray Scattering (WAXS), Grazing–Incidence Small–Angle X–Ray Scattering (GISAXS), Grazing–Incidence Wide–Angle X–Ray Scattering (GIWAXS), Small–Angle Neutron Scattering (SANS), Grazing–Incidence Small–Angle Neutron Scattering (GISANS), X–Ray Diffraction (XRD), Powder X–Ray Diffraction (PXRD), Wide–Angle X–Ray Diffraction (WAXD), Grazing– Incidence X–Ray Diffraction (GIXD) and Energy–Dispersive X–Ray Diffraction (EDXRD) Comparative Study on Malignant and Benign Human Cancer Cells and Tissues under Synchrotron Radiation. Glob Imaging Insights. 2018;3(5):1–10.
107. Heidari A. Nuclear Resonant Inelastic X–Ray Scattering Spectroscopy (NRIXSS) and Nuclear Resonance Vibrational Spectroscopy (NRVS) Comparative Study on Malignant and Benign Human Cancer Cells and Tissues under Synchrotron Radiation. Glob Imaging Insights. 2018;3(5):1–7.
108. Heidari A. Small–Angle X–Ray Scattering (SAXS) and Ultra–Small Angle X–Ray Scattering (USAXS) Comparative Study on Malignant and Benign Human Cancer Cells and Tissues under Synchrotron Radiation. Glob Imaging Insights. 2018;3(5):1–7.
109. HeidariA.CuriousChloride(CmCl3)andTitanicChloride (TiCl4)–Enhanced Precatalyst Preparation Stabilization and Initiation (EPPSI) Nano Molecules for Cancer Treatment and Cellular Therapeutics. J. Cancer Research and Therapeutic Interventions. 2018;1(1):01–10.
110.Gobato R, Gobato MRR, Heidari A. A. Mitra, Spectroscopy and Dipole Moment of the Molecule C13H20BeLi2SeSi via Quantum Chemistry Using Ab Initio, Hartree–Fock Method in the Base Set CC–pVTZ and 6–311G**(3df, 3pd). Arc Org Inorg Chem Sci. 2018;3(5):402–409.
111.Heidari A. C60 and C70–Encapsulating Carbon Nanotubes Incorporation into the Nano Polymeric Matrix (NPM) by Immersion of the Nano Polymeric Modified Electrode (NPME) as Molecular Enzymes and Drug Targets for Human Cancer Cells, Tissues and Tumors Treatment under Synchrotron and Synchrocyclotron Radiations. Integr Mol Med. 2018;5(3): 1–8.
112. Heidari A. Two–Dimensional (2D) 1H or Proton NMR, 13C NMR, 15N NMR and 31P NMR Spectroscopy Comparative Study on Malignant and Benign Human Cancer Cells and Tissues under Synchrotron Radiation with the Passage of Time. Glob Imaging Insights. 2018;3(6):1–8.
113.Heidari A. FT–Raman Spectroscopy, Coherent Anti–Stokes Raman Spectroscopy (CARS) and Raman Optical Activity Spectroscopy (ROAS) Comparative Study on Malignant and Benign Human Cancer Cells and Tissues with the Passage of Time under Synchrotron Radiation. Glob Imaging Insights. 2018;3(6):1–8.
114. Heidari A. A Modern and Comprehensive Investigation of Inelastic Electron Tunneling Spectroscopy (IETS) and Scanning Tunneling Spectroscopy on Malignant and Benign Human Cancer Cells, Tissues and Tumors through Optimizing Synchrotron Microbeam Radiotherapy for Human Cancer Treatments and Diagnostics: An Experimental Biospectroscopic Comparative Study. Glob Imaging Insights. 2018;3(6):1–8.

***Corresponding author:** *Prof. Dr. Alireza Heidari, Ph.D., D.Sc.*
Full Distinguished Professor and Academic Tenure of Chemistry &
Enrico Fermi Distinguished Chair in Molecular Spectroscopy &
Head of Cancer Research Institute (CRI) &
Director of the BioSpectroscopy Core Research Laboratory (BCRL) at Faculty of Chemistry, California South University (CSU), Irvine, California, USA &
Board Member of the World Association of Theoretical and Computational Chemists (WATOC) &
President of the American International Standards Institute (AISI) Irvine, California, USA.
E–mail: scholar.researcher.scientist@gmail.com